Textile Reinforced Concrete for free-form concrete elements: Influence of the binding type of textile reinforcements on the drapability for manufacturing double-curved concrete elements

Shantanu Bhat[1,*], *Matthias* Kalthoff[2], *Patrick* Shroeder[2], *Thomas* Gries[1], and *Thomas* Matschei[2]

[1]Institut für Textiltechnik (ITA) of RWTH Aachen University, Construction Composites Department, 52074 Aachen, Germany
[2]Institute for Building Materials research of RWTH Aachen University, 52062 Aachen, Germany

Abstract. Textile reinforced concrete (TRC) is a sustainable composite material consisting of a cementitious based matrix in combination with an open meshed technical textile reinforcement made of carbon or glass fibres. In the future, TRC could be increasingly used in the form of double-curved concrete elements with the aim of producing filigree yet load-bearing concrete shell structures. To assess whether a textile is suitable as a reinforcement structure in double-curved textile concrete elements, numerous properties need to be investigated and evaluated. The most important of these include good handling properties, bending stiffness tailored to the application, sufficiently pronounced mesh openings, and defect-free drapability. In the course of this work, biaxially reinforced knitted fabrics with five different stitch types (pillar open, pillar closed, tricot counterlaid, tricot closed and plain) were investigated to evaluate the above properties. The draping tests were conducted on a robot-controlled draping test apparatus and evaluated with the aid of an optical measuring system. In addition, the geometric relationship between surface curvature of the double curved elements and the shear angle of different textiles was used to classify the influence of the stitch type on the drapability. Finally, for a given double curved geometry, based on the results the selection of an appropriate textile reinforcement which fulfil the component requirements is carried out and a double curved TRC demonstrator element is prefabricated.

1 Introduction

1.1 Textile Reinforced Concrete

With over 100 million cubic meters used per year in Germany alone, steel reinforced concrete (SRC) is one of the most important building materials of our age [1]. However, due to its high CO_2 emissions, cement production poses a problem to achieve climate targets with a view to a climate-neutral future. Against this background, textile-reinforced concrete (TRC) is coming into focus as a resource-saving composite material. The use of uniform lattice structures made of non-corroding textile reinforcement fibres as an alternative to conventional SRC makes it possible to realize structural components with a thickness of approx. 1 cm and above, thus enabling material savings of up to 80 % and an associated CO_2 saving of up to 50 % [1]. TRC as a building material is also accompanied by the renaissance of the architectural trend of imposing shell constructions, which was lived out until the 1960s, a construction method that was mainly characterized by the architects Felix Candela and Heinz Isler. However, such freeform constructions are no longer economically feasible today with SRC [2,3]. The range of applications for TRC so far include pedestrian bridges, facade slabs, shell roofs (see Fig. 1) and the repair of structures.

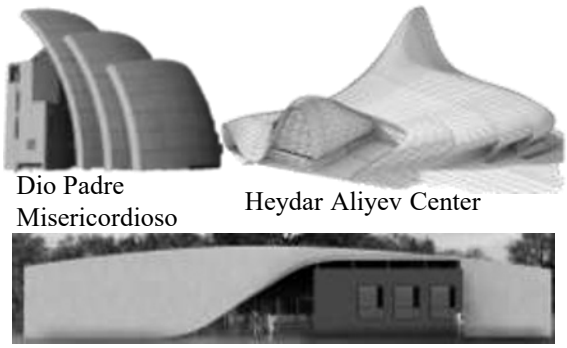

Fig. 1. Free-form architecture buildings

1.2 Textile reinforcements

Similar to SRC, TRC has a grid-shaped reinforcement inserted into it to absorb the tensile forces that occur. Unlike SRC, however, the reinforcement is not steel mesh, but technical textiles. Due to the numerous

* Corresponding author: Shantanu.bhat@ita.rwth-aachen.de

requirements placed on the fibre material (such as alkali-resistant (AR) glass fibres, carbon fibres, aramid fibres, basalt fibres, PVA fibres) have become established for use in the construction industry or in TRC. One of the main advantages of textile semi-finished products in comparison to conventional steel reinforcement is that filigree components can be reinforced in multiple directions with a single planar structure. [5] The characterization of the drapability of warp knitted textile reinforcement structures with different parameters has been carried out until now only with cantilever and shear frame test. [14] The transferability of these test results for different component geometries is not possible. This can be made possible with the help of drape tests, which are investigated within the context of this paper.

1.2.1 Knitted Fabrics

Warp knitting is among the most attractive manufacturing processes for textile reinforcements in the construction industry, as it allows the formation of net-like structures. They are based on the formation and subsequent joining of multiple mesh loops (loops created by yarn bending) [6]. The resulting sheet structures exhibit high drapeability in combination with high elasticity. High-performance yarns are inserted in the loading directions during the production of reinforced knitted fabrics, giving the textile sufficient dimensional stability and increasing the reinforcement properties [6]. A distinction is made between the filler yarn (in the working direction) and the transverse weft (at 90° to the working direction) (see Fig. 2) [8].

1.2.2 Binding types

As defined by DIN EN ISO 4921 (2002) and DIN EN ISO 23606 (2009), the type of binding describes the course of the thread used to form the meshes, which differ in their arrangement and shape. The type of binding influences, among other things, the general reinforcement properties, the penetration possibilities of the concrete and the cross-sectional geometry of the rovings [6]. In warp knitting, numerous binding types exist which can be considered for the textile reinforcement structures. Among the most common basic bindings are: Pillar, tricot and Plain [8]. In addition, so-called combined bindings can be used such as tricot counterlaid, etc. A distinction is made between loose and tight bindings. The Pillar binding compacts the warp yarns the most, resulting in an almost circular cross-sectional geometry. If the binding is rather loose, as in the case of closed tricot, for example, the rovings are less strongly bound and take on a flat and wide shape. The different roving cross sections influence important properties of the textile reinforcement in terms of textile thickness, bending stiffness, strength and drapability [10]. Fig. 2 illustrates these effects.

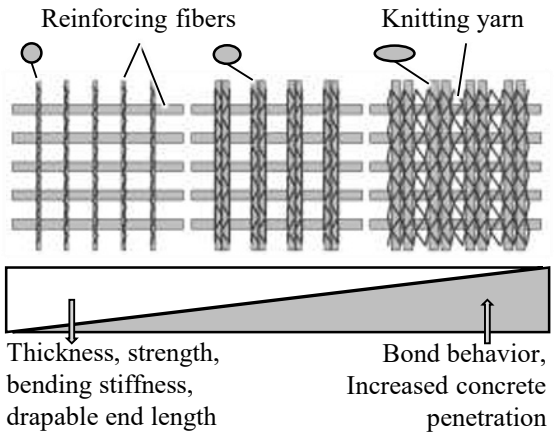

Fig. 2. Nomenclature of warp-knitted fabrics with various binding types and their influence on textile structure [9]

The biaxially reinforced knitted fabrics used for the experiments were produced with the high-performance warp knitting machine “BIAXTRONIC CO” from KARL MAYER Technische Textilien GmbH, Chemnitz, Germany. A total of five different biaxially reinforced knitted fabrics were produced for the tests, which differ only in terms of their binding type (Pillar open, Pillar closed, tricot closed, tricot counterlaid, Plain). An overview of the used textiles can be found in Tab. 3.1. The parameters fibre, fibre fineness, warp and weft repeat and stitch length were kept constant in order to be able to investigate the pure influence of the binding type on the textile properties.

Table 1. Overview of the different textiles used

		Pillar open	Pillar closed	Tricot closed	Tricot counterlaid	Plain
Frontside				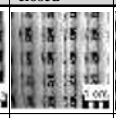		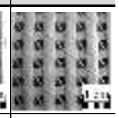
Backside		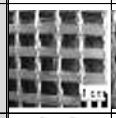			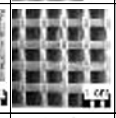	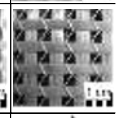
Sketch		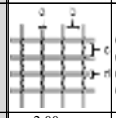	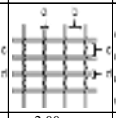	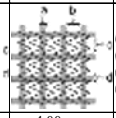	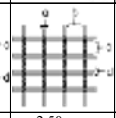	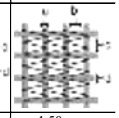
Dimensions	a	2,00 mm	2,00 mm	4,00 mm	2,50 mm	4,50 mm
	b	6,00 mm	6,00 mm	4,00 mm	5,50 mm	3,50 mm
	c	4,25 mm	4,25 mm	4,25 mm	4,25 mm	4,25 mm
	d	3,75 mm	3,75 mm	3,75 mm	3,75 mm	3,75 mm

The used rovings are made of AR glass type Cem-FIL 5325 from Owens-Corning Fiberglas Deutschland GmbH, Frankfurt, Germany and have 2400 tex fineness. The influence of other parameters, such as mesh row spacing, knitted yarn tension or fibre stock, has been intensively investigated within the framework of SFB 528 and 532; the parameters are presented as examples in [5,9].

1.3 Drapability

Drapability is described as the property of two-dimensional textile semi-finished products to adapt to given three-dimensional geometries by external forces [10]. Generally speaking, in the case of textile semifinished products, there is a pronounced correlation between drapability and dimensional stability. As a rule, the lower the dimensional stability and bending stiffness, the better the drapability. During the draping of textile fabrics, the mechanical properties, the impregnation properties with the matrix and the reinforcement properties can change [10,11]. This is due to the fact that the adaptation of a textile semi-finished product to a double-curved geometry usually takes place under the influence of external forces. These forces are triggers for local changes such as changes in fibre or yarn orientation at the fibre and roving level. They are referred to as deformation mechanisms. The changes caused at the level of the textile semi-finished product due to these deformation mechanisms are called drape effects or drape errors. These changes are mostly plastic, so they cannot be reversed later and result in a deterioration of the mechanical properties of the reinforcement structure. [10,11].

Draping effects (Fig. 3) that occur within the textile surface result mainly from the unavoidable fibre displacements during draping [12]. These two-dimensional draping effects include undulations and gaps.

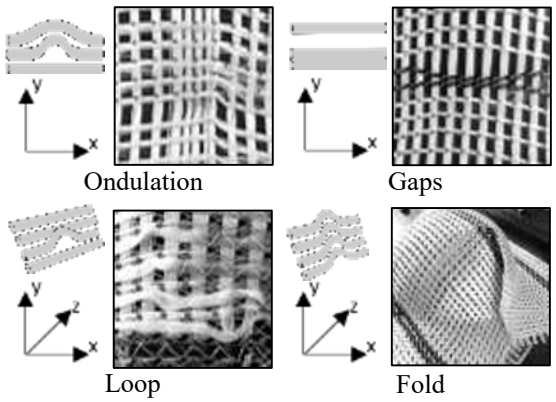

Fig. 3. Drape effects occurring in biaxial textile reinforcements

Undulations are the consequences of buckling of the rovings [12]. If drape effects emerge from the textile surface, they are called three-dimensional drape effects. Folds are characterized by the fact that on a certain section in the textile, both the rovings in the direction of production and those running against the direction of production stand out from the drape geometry [12]. The difference between fold formation and loop formation is that the external force that causes buckling and thus the formation of loops is not large enough to cause a proper fold to form, but only causes individual rovings to protrude from the textile surface [13].

1.4 Geometrical component design

In civil engineering, the shell construction method is not a new achievement. As early as the 1930s, more and more work was done with components that functioned both architecturally and mechanically by curving or folding [3]. In particular, the use of double-curved concrete structural members is versatile. Hyperbolic paraboloids, conoids and rotational hyperboloids are examples of such relevant developable surfaces. These surfaces can be differentiated using the Gaussian curvature [13]. In order to be able to describe three-dimensional shapes more quickly and intuitively, Koenderink introduced the so-called Shape Index [13]. This dimensionless index ranges from -1 to 1. Shapes with a shape index of -1.0 and 1.0 have principal curvatures of the same sign, while a shape index of 0.0 describes different signs of the principal curvatures [13].

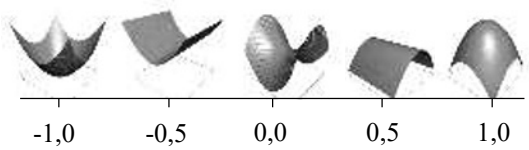

Fig. 4. Characteristic shape with respective shape indexes following [15]

Developable ruled surfaces (e.g., cylinders) can be generated by pure bending of a two-dimensional rectangular surface. Double curved surfaces cannot be generated by simply reshaping a rectangular two-dimensional surface, since the Gaussian curvature in the deformed state is non-zero and thus no longer constant. However, an exception to the Gaussian rule put forward by Schipper in his work is the forming of materials with low extensional stiffness. This follows that deformation of a rectangular planar surface can occur either by stretching in the x- and y-axis directions or by shearing in the x,y-axis direction [13]. In this context, Schipper [13] has designed a model-based approach to describe the geometric relationship between a deformed and an undeformed planar structure. This mathematical model from Schipper has been used in the context of this work for the draped textile geometries. The underlying algorithm results in a mathematical grid which is similar to the textile reinforcement grid. This Grid contains angles at which the individual rovings theoretically intersect in the deformed textile. The resulting angle in each case is the 90° angle, reduced (or increased) by the shear angle, which exists between the rovings in the undraped state. For the evaluation and determination of the necessary shear angles depending on the chosen geometry, the relation between the Gaussian curvature and the shear angle established by Calladine is used (see equation (1) [13].

$$\beta = (n \cdot \mathrm{K} \cdot c^2 \cdot 360°) / 4\pi \qquad (1)$$

β = shear angle in degrees, K = Gaussian curvature in m^{-2}, c = fixed grid length in m and n = grid cell

considered. The shear angle must be determined anew for each grid cell. The coefficient n accounts for the fact that the shear angle increases with increasing distance from the origin [13]. This coefficient can be determined for the individual grid cells defined by i and j using equation (1).

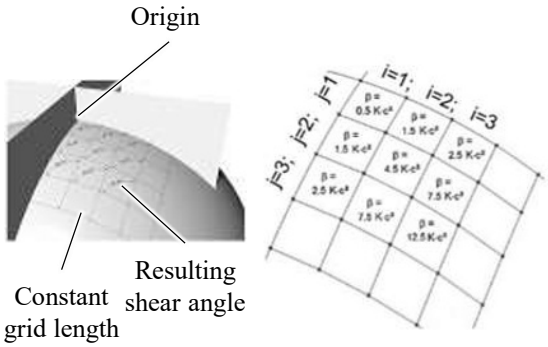

Fig. 5. Parametric modelling approach for creating a grid on a double curved surface

2 Experimental Investigation

2.1 Experimental setup and execution

The aim of drape test methods is to measure and evaluate the drape behaviour of textiles with regard to the deformation mechanisms and drape effects described above, taking into account the requirements relevant for industry and the cross-component relevance of the textiles to be tested [11]. For the draping of biaxial open meshed textiles, no standardized test method exists yet. . Fig 6. shows the draping test rig used for the experiments.

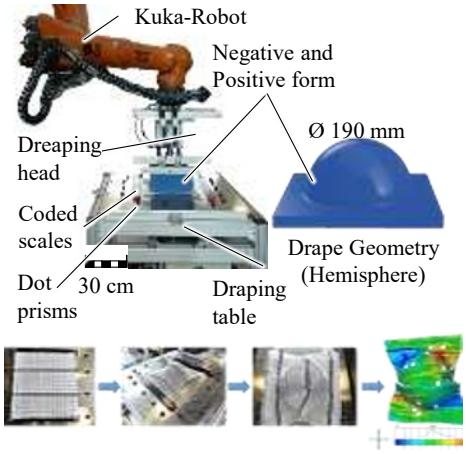

Fig. 6. Illustration of the draping of textiles with the test rig used for the experiments

For this reason, there have already been attempts to use drape test methods for woven fabrics and multiaxial fabrics from the automotive industry.

The test rig designed at ITA consists of a demountable frame structure to which the positive mould half of the draping geometry is attached. The negative counterpart is attached to a specially made fixture on a Kuka robot "KR 150-2" from KUKA Robotics AG. The working principal is illustrated in Fig. 7.

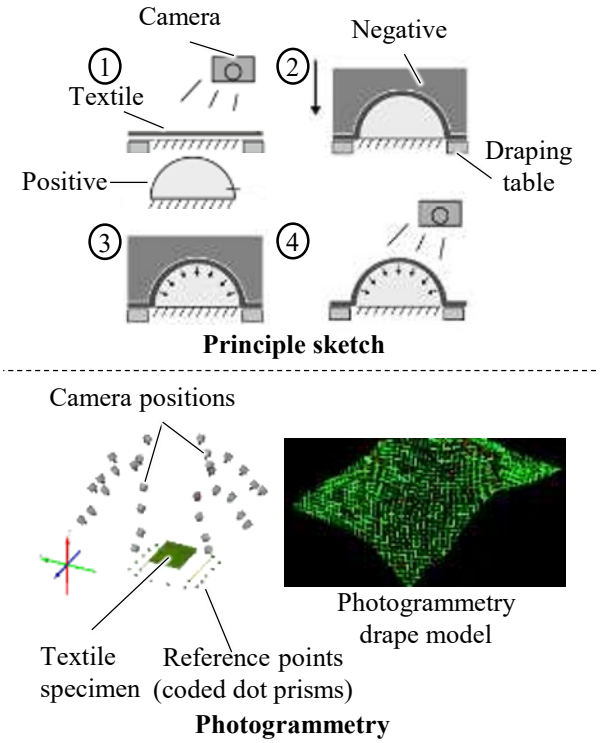

Fig. 7. Working principle and interface of the ARGUS software

The modular design of a drape test rig also allows a wide variety of standard geometries to be exchanged. The most common geometries include the simple hemisphere, the stretched hemisphere, the double dome and the pyramid with a square base. Standard geometries differ in the number of symmetry planes present and the arrangement of varying degrees of local curvature [11]. The selection of the geometry follows criteria such as the application or even the anisotropic shear behaviour of the textile [11]. The hemisphere drape geometry used in the framework of this study is a widely used geometry for performing drape tests, because it makes it easy to perform analysis of the drapeability of textiles, since textile deformations occur independently of the orientation of the textile. [11,13].

For the drape tests, the textile specimens were cut square. The specimen dimensions were 400 mm in length and width. These dimensions were selected on the basis of the used drape geometry and its dimensions. Five specimens for each binding type were tested. In order to be able to evaluate a draping result with sufficient significance, a computer-aided optical measuring system is usually employed, which allows an accurate evaluation of the shear angle distribution characteristic of a textile. Photogrammetry is the measuring technique adopted for this work. It is based on the fact that a large number of photos are taken from different angles before and after the textile is draped, allowing the geometric shapes and position of the textile

semi-finished products to be digitally recorded. Fig. 7 shows the three-dimensional image of the textile specimen based on it. A regular pattern of red dots marked on the textiles is used to help capture the exact coordinate shifts of individual points before and after the draping process based on the captured images. The ARGUS-GOM system from Gesellschaft für Optische Messtechnik GmbH, Braunschweig, Germany, was used for the experiments.

3 Presentation and Discussion of results

The ARGUS software allows the evaluation of the acquired data by recognizing and including the relevant quantities for the drape analysis. These include the shear angle, the strain in the fibre direction, the strain perpendicular to the fibre direction and the distance to the surface. It should be noted here that the strains detected by the measurement system are not real roving strains due to the forces being too small, but local formations of loops, alleys and folds [11]. This is the reason why an optical evaluation without the aid of software was carried out additionally to determine the occurring drape effects.

3.1 Evaluation with ARGUS System

The ARGUS software created a three-dimensional image of the textile and coloured the individual areas according to the shear angle formation (see Fig. 8).

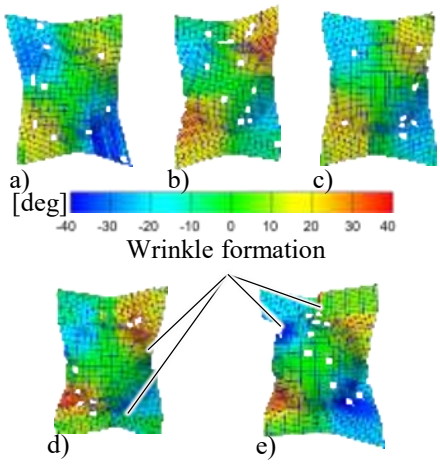

Fig. 8. ARGUS analysis plots: a) Pillar open, b) Pillar closed, c) Tricot counterlaid, d) Tricot closed, e) Plain

A distinction was made between a predefined positive or negative shear angle. In positive shear, a body is deformed in a clockwise direction, while in negative shear, deformation takes place in an anticlockwise direction. As can be seen from Fig. 8, the basic shear angle distribution is very similar for all specimens.
In the x- and y-axis directions of a coordinate system having the origin at the hemisphere centre, the shear angles are very small or even zero. This can be explained by the fact that shear stress only occurs when the force required to drape a textile onto a double-curved surface does not act in the roving direction. For example, if the drape geometry is only single-curved, no shear angles will form in the textile, because the rovings are only stressed in pure bending. A similar effect was observed in these tests on the two main axes.

Positive shear angles were formed on the diagonals at a 45° angle (counter clockwise) to the x-axis, and negative shear angles on the axis at right angles to this. The very small shear angles after complete draping in the tricot closed and plain binding types were due to the formation of folds. In Fig. 8, the strong wrinkle formation in the plain binding and the less strong wrinkle formation in the tricot closed binding can be seen. Fig. 9 illustrates the main results of the shear angle investigation. For the open pillar bond, maximum shear angles of 38° were measured. The maximum shear angle for the closed pillar and reverse tricot bindings was 29° and 27° respectively, and for the closed plain and tricot bindings 34°.

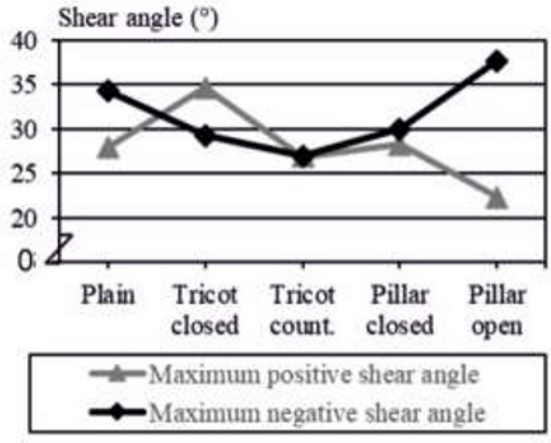

Fig. 9. Shear angle formation in the tested textiles

All specimens, with the exception of the specimens with the reverse tricot and closed pillar bond, exhibited a strongly anisotropic shear behaviour, i.e., a non-uniform formation of negative shear angles compared to positive shear angles (see Fig. 4.4 and Fig. 4.5). This effect can be explained by the binding type alone since the used drape geometry (hemisphere) has no influence on the anisotropic shear behaviour due to the double-symmetric shape.

The knitting yarn behaviour can be explained most easily using the example of the plain binding. Here, the warp knitted yarn, which runs approximately at a 40° angle to the direction of manufacture in the knitted textile was stretched under positive shear stress, while it was less stretched under negative shear and even compressed in places. If the stretched knitted filament did not fail, a certain point was reached at positive shear where the

knitted filament hindered or completely prevented further roving rotation that would cause larger shear angles to occur. This probably explains why the maximum positive shear angle of about 28° is smaller than the maximum negative shear angle of 34°. Similar effects were observed with the closed tricot binding, the only difference to the plain binding being the warp knitted thread running approximately at 45° to the direction of manufacture and not a 40° as for the plain binding.

Regarding the critical shear angle, only limited specific statements can be made based on the drape tests alone. The results of the optical evaluation of the drape tests show that the critical shear angle is reached in a closed manner, at least for the plain and tricot bindings as occurrence of folds was observed. Since the maximum measured negative shear angle for the pillar binding is greater than that for the plain and tricot closed bindings, the critical "negative" angle of shear is also greater for the samples with the pillar binding which can be draped almost without defects.

3.2 Optical evaluation

As already stated in section 3.1, not all drape errors could be detected by means of the ARGUS graphics. Thus, the optical evaluation is necessary to determine the correlations between shear angle and drape defects. Fig. 10 shows the frequencies of the occurring draping errors for the five specimens for each binding type.

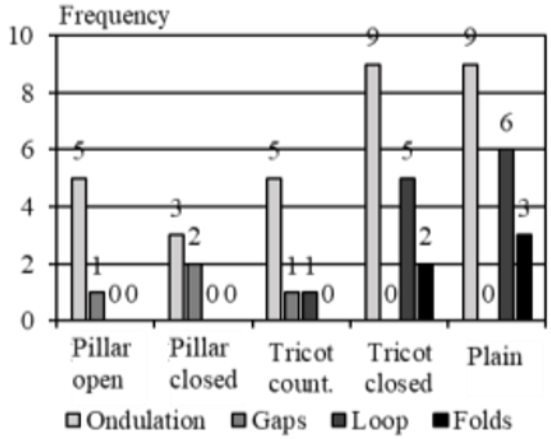

Fig. 10. Overview of optical evaluation of drape errors

The following statements can be drawn from optical evaluation:
- The binding type significantly influences the formation of the various draping effects.
- The bindings tricot closed and plain show more or less pronounced wrinkling, which reduces the drape quality.
- Wrinkling does not occur
- Cross-connections of the rovings in the bindings tricot closed and plain prevent roving displacement parallel to the warp direction.
- Both pillar bindings can be draped almost faultlessly.

3.3 Comparative evaluation of the calculated and measured shear angles

The comparison of the calculated shear angles based on the mathematical model from Schipper, with the results of the experimental determination of the shear angles with the ARGUS software illustrates that the measured shear angles partly deviate from the calculated ones. This observation does not require an exact calculation since an isotropic shear behaviour results from the model when applied to one hemisphere. This is in contradiction with the mostly anisotropic shear behaviour of the considered textiles determined through the drape tests. The nature, magnitude and reason for the discrepancies are explained below. The evaluation graphs from the ARGUS software were used to accurately determine the measured shear angles, which were viewed at 5° intervals (see Fig. 4.9).

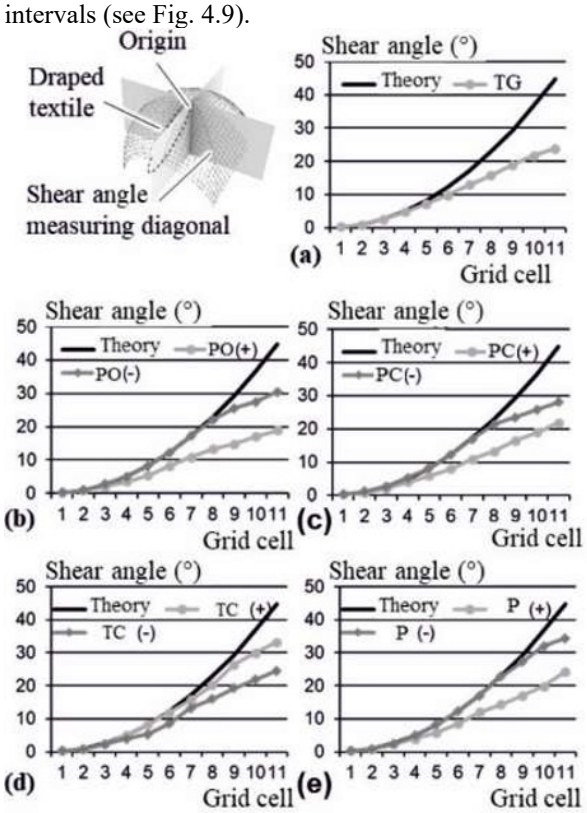

Fig. 11. Evaluation model for the shear angle distribution and comparison of theoretical and measured shear angles. a) Tricot counterlaid, b) Pillar open, c) Pillar closed, d) Tricot closed, e) Plain

Analogous to the algorithm, a regular grid, which in this case is equal to the point grid (8 x 8 mm), was selected and placed on each graph. Then the shear angle was read with the help of the colouring in the considered grid cell. The evaluation of the shear angles was carried out by considering only the two main diagonals (marked in Fig.11) at an angle of 45° to the construction planes.

The largest shear angles are formed on the main diagonals, which makes them the most interesting for the

comparison of the individual binding types. Fig. 11 illustrates the differences between the theoretically calculated and measured shear angles for all the five binding types studied. Since all considered grid cells are located on the main diagonals, e.g., the entry 3 on the x-axis means that the grid cell $i = 3$ and $j = 3$ is considered. The consideration ends at the 11 grid cell, because here the radius of the hemisphere is reached with the chosen grid spacing of 8 mm. It is noticeable that the deviations between the theoretically calculated and measured shear angles increase with increasing distance from the origin or with larger shear angles. In general, the measured shear angles are smaller than the calculated shear angles. Moreover, for each type of binding with an anisotropic shear distribution there is a curve that fits much better to that of the theoretically calculated shear angles.

Depending on the type of binding, this is true for either positive or negative shear. This is in line with the influence of the knitted yarn on the roving rotation and thus on the size of the shear angles formed. For example, the open pillar binding under positive shear, the roving rotation is already hindered by the knitted yarn at low shear angles, which causes the curve with the measured shear angles to separate early from the curve of the theoretically calculated ones. The situation is different with negative shear, where this phenomenon only becomes apparent from the eighth grid cell onwards.

4 Discussion and conclusions for the choice of a suitable textile reinforcement

In the table below the requirements for textile reinforcement are listed, based on which the suitability of textiles as reinforcement structure is evaluated (see Table. 3). These categories are selected from the perspective of a precast factory and the quality standards to be fulfilled for the TRC panels. The listed degrees of fulfilment refer to components which have the same or similar geometry aspects as those to which the drape test refers. Based on the degree of fulfilment of the different textiles as reinforcement in double-curved components, the tricot closed (TC) and plain (P) bindings can be sorted out because the drape quality is not given here. Compared to the closed pillar (PC) binding, the tricot counterlaid (TG) binding and open pillar (PO) binding do not fulfil the criterion of mesh opening in the same way. For the closed pillar (PC) binding, a degree of fulfilment of 88% can be assumed based on all criteria and is thus selected as the suitable textile reinforcement

Table2. Rating of the textile reinforcements

	PO	**PC**	**TG**	**TC**	**P**
Handling	◔	◔	◔	◕	◕
Shape deviation	◔	◔	◔	●	●
Mesh opening	◔	●	◔	◕	◔
Drape quality	◔	◔	◔	○	○
Fulfillment (%)	75	**88**	75	38	50

○ Unsuitable ◕ Rather unsuitable
◔ Rather suitable ● Suitable

5 Implementation and production of a double curved-textile reinforced concrete component

For the demonstrator component to be fabricated in this work, a thin-walled, double-curved façade panel made of TRC is chosen. Fig. 12 (a) shows the selected demonstrator component as a possible facade element. The dimensions of the base area of the component are 400 by 600 mm. The curvature distribution, see Fig. 12 (b) was chosen to observe the behaviour of the textile with respect to a change in Gaussian curvature and with respect to a transition between a concave and a convex section of the component, which is particularly popular for free-form façade elements. Fig. 12 (b) also shows the theoretical shear angle formation for the demonstrator. The largest theoretical shear angles with up to 33° are to be expected at the transitions between positive and negative Gaussian curvature. Material jams and fitting inaccuracies could also occur at these points. Considering the drape analysis results from the experiments, the closed pillar textile reinforcement with a maximum shear angle of 29° should be suitable for the curvature of the demonstrator component.

5.1 Fabrication of a double curved TRC panel

The ready-mixed mortar mixture StoCrete TG 203 from StoCretec GmbH, Germany, was used as the fine concrete mixture. The lamination process was selected for the fabrication of the demonstrator component. The aim was to produce a filigree component consisting of three concrete layers and 2 textile layers. Fig. 12 shows the precast demonstrator component from above and from the side. The component showed no visible defects with regard to cracking and textile displacement. There were slight variations in component thickness at the edges.

Thus, using the drapability analysis proposed in this paper, a component specific selection of textile reinforcement for freeform concrete panels is now

possible. This enables the selection of the textile reinforcement with appropriate textile parameters. Thereby ensuring not only textile positioning but also good concrete penetration and good handling of the textile during precasting.

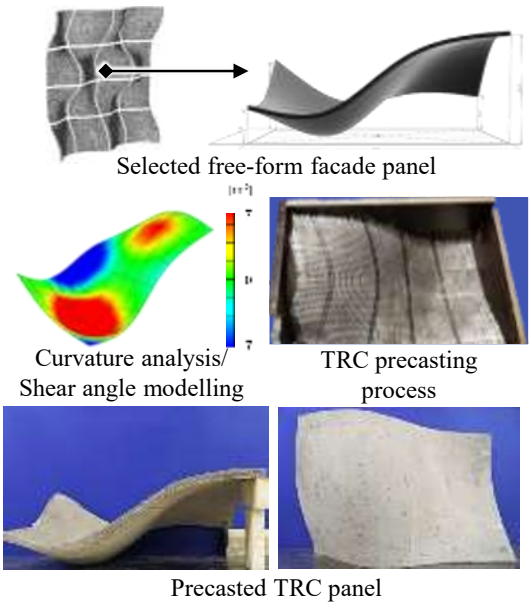

Fig. 12. Design and Fabrication of the free-form TRC panel

6 Conclusion

In the course of this work, biaxially reinforced knitted fabrics with five different binding types (pillar open, Pillar closed, tricot counterlaid, tricot closed and plain) were investigated to evaluate the properties good handling, sufficiently pronounced mesh openings, and defect-free drapability. The type of binding significantly influences the magnitude and distribution of local shear angles. The formation of drape defects is influenced by the knitted yarn characteristic of a binding type and the associated restricted freedom of movement of the rovings. At almost 40°, the open pillar binding exhibited the highest shear angle formation and thus the smallest lattice openings. The bindings tricot closed and plain showed pronounced wrinkling and are thus unsuitable as textile reinforcement in components with similar geometry. An almost faultless drapeability could be achieved in the specimens with the bindings pillar and tricot in opposite directions. The double-curved textile concrete demonstrator component fabricated consisted of three layers of concrete approximately 0.5 cm thick and two layers of meshed textile reinforcements closed with the pillar type of binding. The pillar binding open meshed textile reinforcement was able to take the demonstrator component shape without any drape effects.

References

1. C. Gärtner, Was ist Carbonbeton?: Was ist Carbonbeton?, *Carbon Concrete Composite e.V., (2019)*
2. R. Schützeichel, *Symp. zu Candela, Isler und Müther an der ETH Zürich*, (Die Schalenbauer BDA, der Architekt, (2018)
3. C. Schätzke, H. Schneidr, T. Joachim, M. Feldmann M, D. Pak, J. Geßler, J. Hegger, A. Scholzen. Doppelt gekrümmte Schalen und Gitterschalen aus Textilbeton. *Kolloquium zu textilbewehrten Tragwerken, **CTRS6**, (2011)*
4. M. Curbach, F. Schladitz, E. Müller, Carbon concrete - from research to real life. *BFT International,* 1, S. 36-41, (2017)
5. T. Gries, S. Janetzko, P. Kravaev, Textile Verstärkungsstrukturen, Übersicht der Forschungsaktivitäten im Rahmen des SFB 532 *Curbach M., Ortlepp R., Kolloquium zu textilbewehrten Tragwerken **CTRS6***, (2011)
6. C.Cherif, Textile Prozesskette und Einordnung der textilen Halbzeuge, *CHERIF, CH. (Hrsg), Textile Werkstoffe für den Leichtbau, Springerverlag, Berlin, Heidelberg,* (2011)
7. T. Gries, M. Raina, T. Quadflieg and O. Stolyarov, Manufacturing of textiles for civil engineering applications, *In Thanasis Triantafillou, Textile Fibre Composites in Civil Engineering, Woodhead Publishing Series in Civil and Structural Engineering,* **60**, (2016)
8. V. Eckers, Multiscale analysis of grid textile structures for textile-reinforced concrete., Aachen, *Techn. Hochsch., D*, (2012)
9. P. Ermanni, Composites Technologien, *ETH Zürich*, (2007)
10. H. Krieger, Methode zur Auslegung von Gelegen mit lokal angepassten Fertigungsparametern für Hochleistungs-Faserverbundkunststoffe, *Technische Hochschule Aachen, Dissertation, Shaker Verlag,* (2015)
11. M. Christ, Definition und Quantifizierung der Drapierbarkeit von multiaxialen Gelegen durch die Vermessung von Einzeleffekten, *Bremen PhD Thesis*, (2018)
12. D. Lordick, D. Klawitter, M. Hagemann Liniengeometrie für den Leichtbau, *Scheerer S., Curbach M., Leicht bauen mit Beton, Forschungen im Schwerpunktprogramm 1542, Technische Universität Dresden*, (2014)
13. R. Schipper, P. Eigenraam, Mapping double-curved surfaces for production of precast concrete shell elements. *Heron*, **61 (3)**, 211-233, (2016)
14. G. Dittel, The world's first double-curved textile concrete facade, *Institut für Textiltechnik of RWTH Aachen University*, (2019)